IRis

Northeastern University

Research Thrust R2 Presentations

CenSSIS Research Thrust R2: Physics Based Signal Processing and Image Understanding

January 01, 2007

MDL Principle Applied to Dendrites and Spines Extraction in 3D Confocal Images

Xiaosong Yuan
Rensselaer Polytechnic Institute

Badrinath Roysam
Rensselaer Polytechnic Institute

Recommended Citation

Yuan, Xiaosong and Roysam, Badrinath, "MDL Principle Applied to Dendrites and Spines Extraction in 3D Confocal Images" (2007). *Research Thrust R2 Presentations.* Paper 26. http://hdl.handle.net/2047/d10008858

This work is available open access, hosted by Northeastern University.

MDL Principle Applied to Dendrites and Spines Extraction in 3D Confocal Images

Rensselaer Polytechnic Institute, Troy, NY 12180
Xiaosong Yuan and Badri Roysam

Abstract

The structure of neuronal dendrites and dendritic spines has been realized to reveal many important aspects of cognitive functions. We present an MDL (Minimum Description Length) principle based algorithm to identify the morphologic structure of dendritic branching and analyze spine density and distribution. An algorithm utilizing the gradient vector field to locate the skeletons of the tubular objects is applied after an anisotropic diffusion process. In order to generate a graph structure from the 3D skeleton, a minimum spanning tree algorithm based on density weighted edges (DW-MST) is employed. MDL models are created and optimized under consideration of the tree branches in dendritic structure. We have the prior probabilities of the dendritic spines, which should be involved in the descriptive language. In the MDL strategy, the spine features are investigated and considered as the observed data for any given models. We choose the models that minimizes the number of bits required to describe the features given the model plus the number of bits required to describe the model. Many experimental results show the efficiency of our algorithms on 3D fluorescence images.

1. Introduction:

Important aspects of cognitive function are correlated to dendritic branching morphology and spine density and distribution. The morphologic variation of dendrites and spines distribution can be analyzed to predict the function of neural networks.

Dendritic spines are small protrusion objects from the dendritic backbones. Due to other non-spine artifacts from digitization effects, segmentation errors, spurious cell debris, etc., the spines have to be recognized among all other spurs.

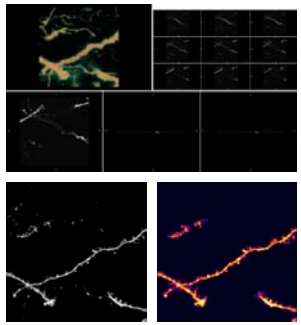

(a)

(b), (c)

Figure 1. (a) Original 3D confocal microscopy neuronal image; (b) 3D image after deconvolution. It is projected to 2D along z-direction. (c) Prepocessed 3D image.

2. Preprocessing and Anisotropic Diffusion

The 3D density map after thresholding is irregular on the isosurface, a certain amount of dilation process can improve it. We assume the tubular objects are not hollow inside, therefore a flood filling process is applied to the volume then. Also there are a lot of isolated small objects which are from the thresholded background. We can use connected components labeling and removal to remove them.

Anisotropic diffusion can smooth out some unwanted small objects attached to the main part of the tubular objects. It is an iterative method and can gradually produce smooth results as requested. $\frac{\partial I(x,y,t)}{\partial t} = \nabla \bullet \{D(x,y)\nabla I(x,y,t)\}$

where $D(x,y) = \exp\left\{-\left|\frac{\nabla I(x,y)}{k}\right|^2\right\}$

3. Critical Points and Skeletonization

The gradient vector filed can be computed from the 3D density map with a derivative kernel. By analysis of the gradient vector field, we can locate the critical points, which include attracting points, repelling points and saddle points.

The saddle points found above can be used as the seeding points. Following the streamline from the seed points will proceed to the attracting points, which are the peak points of the density map. The saddle points and attracting points are located on the skeletons. The streamlines between them are the skeletons we are concerned.

In order to extract all possible spines, high curvature points should also be included as seeds. The tube ends may correspond to high curvature points in the gradient vector field.

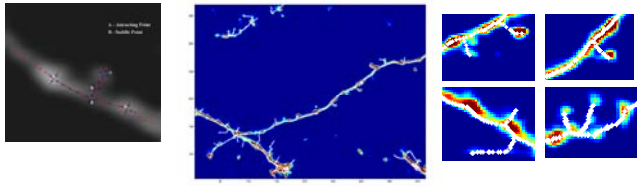

(a) (b) (c)

Figure 2. (a) Critical points and connection; (b) Skeletons of dendrite and spines represented in 3D points (shown in white dots); (c) Magnified parts in (b).

4. Graph Morphology

4.1 Density Weighted Minimum Spanning Tree (DW-MST)

If we denote the vertices as V_i, $i = 1,..,N$. and the edge between vertex i and j as E_{ij} , we can compute the edge weight in the following density weighted way.

$$E_{ij} = d(V_i, V_j)\left|\frac{2}{f(V_i) + f(V_j)}\right|$$

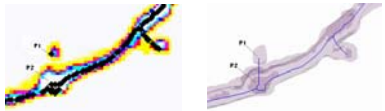

Figure 3. Detection of Detached Spines. (a) 3D Skeleton points (black dots) of part of dendrites. (b) DW-MST from the 3D skeleton points represented by vertices and edges.

4.2 Graph Morphology Methods

Graph erosion operation can change the morphology of the graph and remove unwanted trivia leaves of the tree and keep the major tree structure.

$$Erosion(G) = G - \bigcup_i \{\{e_i, v_i\} \mid dgr(v_i) = 1, e_i = edge(v_i), (e_i, v_i) \in G\}$$

5. MDL principle on dendritic and spine structure

In the MDL criteria function, we aim to optimize on the two terms, each of which can have different forms according to our purpose.

$$\hat{M} = \arg\min_{M_i}\{|L_c(D \mid M_i)| + |L_m(M_i)|\}$$

(1) Description of Data with the hypothesis. $|L_c(D \mid M_i)| = -\log_2 P(D \mid M_i) = -\sum_{x \in \text{nodes of } M_i} \log_2 P(D(x) \mid M_i)$

(2) MDL model M_i. Consider the topology of the dendritic structure and use tree branches.

(a) No prior knowledge

when the total number of spines is n, the model description length is nc.

$$|L_m(M)| = \sum_{i \in B} |L_m(M_i)| = nc$$

(b) Prior knowledge

we consider the spines are protruding from backbones only and the protruding positions are close to the backbones.

$$L_m(M) = L_m(M_1, M_2, ...M_N) = \sum_i (\beta \cdot d(M_i, B) + \gamma)^{M_i}, \quad \beta > 0, \gamma > 1$$

Spine density restriction states the neighboring two spines are not intending to be too close to each other; otherwise it can be a false detection.

$$L_m(M) = L_m(M_1, M_2, ...M_N) = \mu \sum_i \sum_{j \neq i} I_\theta(d(M_i, M_j)) \quad \theta = \{x \mid 0 \le x \le \delta\} \quad \mu > 0$$

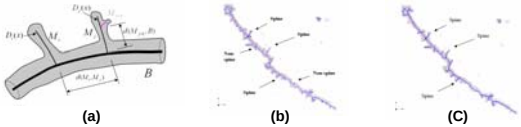

(a) (b) (C)

Figure 4. (a) Spine MDL model (b) Skeleton obtained from DW-MST (C) its MDL representation. Figures (b) and (c) give a comparison of the spine extraction without MDL (skeleton only) and with MDL principle

6. MDL Criterion on Spine Features

The first term of MDL criterion is derived from the distribution of feature vectors, which is assumed to be multi-variable Gaussian distribution.

$$|L_c(D \mid M_i)| = -\sum_{x \in M} \log_2 P(D(x) \mid M_i) = N \cdot b + a \sum_{x \in M} \left((D(x) - \hat{u}_M)' \, \Sigma_M^{-1} (D(x) - \hat{u}_M)\right)$$

The MDL criterion function L(M) of the spine models can be expressed as

$$L(M) = |L_c(D \mid M)| + |L_m(M)| =$$
$$N \cdot b + a \sum_{x \in M} \left((D(x) - \hat{u}_M)' \, \Sigma_M^{-1} (D(x) - \hat{u}_M)\right) + \sum_i (\beta \cdot d(M_i, B) + \gamma)^{M_i} + \mu \sum_i \sum_{j \neq i} I_\theta(d(M_i, M_j))$$

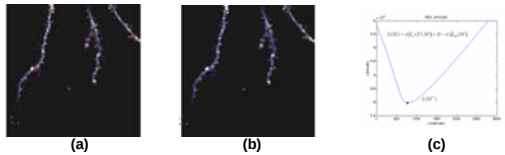

(a) (b) (c)

Figure 5. . MDL representation with different levels of conciseness (a) and (b). The extreme case of conciseness reduces to no spine at present. (c) MDL optimum

7. Experimental Results

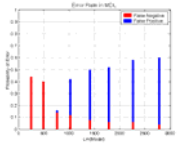

Figure 6. Error rates in MDL at various levels of conciseness.

Evaluation of Algorithm	Num of Spines	Missing Rate	False Detection
Time series 6A	245	14.2%	20
Time Series 7A	120	16.6%	5
Time Series 8A	95	10.5%	45
Time Series 11A	160	8.8%	20
Time Series 14A	205	12.2%	35

Table 1. Evaluation of algorithm

8. Summary

We applied anisotropic diffusion to the confocal microscopy images and locate critical points. The MDL principle plays an important role in the tradeoff between coverage and conciseness and prior knowledges of spines are considered and translated into the MDL language. The spines and non-spine branches can be identified with low error rate.

9. Acknowledgement

We are thankful to Prof. Joshua Trachtenberg for all of the datasets in this presentation. This work was supported in part by CenSSIS, under the Engineering Research Centers Program of the NSF.

April 19, 2007 © Copyright Reserved